Predatory selection of mucoid, antibiotic resistant *Pseudomonas putida* phenotype by myxobacterium *Cystobacter ferrugineus*

Shukria Akbar[a] and D. Cole Stevens[a,#]

Department of BioMolecular Sciences, University of Mississippi, University, MS, USA[a]

Running Head: Predatory selection of antibiotic resistant *P. putida*

#Address correspondence to D. Cole Stevens, stevens@olemiss.edu.

Abstract: Predation contributes to the structure and diversity of microbial communities. Predatory myxobacteria are ubiquitous to a variety of microbial habitats and capably consume a broad diversity of microbial prey. Predator-prey experiments utilizing myxobacteria have provided details into predatory mechanisms and features that facilitate consumption of prey. However, prey resistance to myxobacterial predation remains underexplored, and prey resistances have been observed exclusively from predator-prey experiments that included the model myxobacterium *Myxococcus xanthus*. Utilizing a predator-prey pairing that instead included the myxobacterium, *Cystobacter ferrugineus,* with *Pseudomonas putida* as prey, we infrequently observed surviving phenotypes capable of eluding predation. Comparative transcriptomics between *P. putida* unexposed to *C. ferrugineus* and the survivor phenotype suggested that increased expression of efflux pumps, genes associated with mucoid conversion, and various membrane features contribute to predator avoidance. The *P. putida* survivor phenotype was confirmed to be resistant to the antibiotics kanamycin, gentamicin, and tetracycline and to produce more alginate than predator-unexposed *P. putida*. Unique features observed from the survivor phenotype including small colony variation, efflux-mediated antibiotic resistance, and increased mucoid conversion overlap with traits associated with *Pseudomonas aeruginosa* predator avoidance and pathogenicity. The survivor phenotype also benefited from increased predator resistance during subsequent predation assays. These results demonstrate the utility of myxobacterial predator-prey models and provide insight into prey resistances in response to predatory stress might contribute to the phenotypic diversity and structure of bacterial communities.

36 **Introduction**

37 Abundant within soils and marine environments, predatory myxobacteria contribute to
38 nutrient cycling within the microbial food web (Findlay, 2016; Munoz-Dorado et al., 2016;
39 Albataineh and Stevens, 2018; Mohr, 2018). Myxobacteria are prolific producers of
40 antimicrobial specialized metabolites and display a cooperative, swarming predation
41 strategy that can be readily reproduced and monitored within laboratory settings making
42 them uniquely appropriate for assessment of predator-prey interactions (Munoz-Dorado
43 et al., 2016; Albataineh and Stevens, 2018; Mohr, 2018; Nair et al., 2019). Broadly
44 considered generalist predators, myxobacteria capably predate a range of prey including
45 both Gram-negative and Gram-positive bacteria as well as fungi (Perez et al., 2016; Nair
46 et al., 2019). Constitutive production of specialized metabolites and lytic proteins are often
47 associated with this predatory range, and a variety of metabolites and enzymatic features
48 have been reported to benefit predation (Xiao et al., 2011; Muller et al., 2016; Livingstone
49 et al., 2018; Ellis et al., 2019).

50 However, relatively few examples of prey resistance to myxobacterial predation have
51 been reported (Sutton et al., 2019). Compared to features associated with bacterial
52 strategies to avoid protozoan predators, prey avoidance of predatory myxobacteria
53 remains underexplored (Weitere et al., 2005; Justice et al., 2008; Erken et al., 2013; Seiler
54 et al., 2017; Sun et al., 2018). Examples of prey responses correlated with resistance to
55 myxobacterial predation include *Escherichia coli* biofilm formation (DePas et al., 2014),
56 *Bacillus subtilis* sporulation and production of bacillaene (Muller et al., 2014; Muller et al.,
57 2015), *Bacillus licheniformus* glycosylation of the predation-associated metabolite
58 myxovirescin A (Wang et al., 2019), galactoglucan exopolysaccharide production and

59 increased melanin production by *Sinorhizobium meliloti* (Perez et al., 2014; Contreras-
60 Moreno et al., 2020), and formaldehyde secretion by *Pseudomonas aeruginosa* (Sutton
61 et al., 2019). All of these features were discovered from predator-prey experiments
62 utilizing the model myxobacterium *M. xanthus*.
63 We suspect the development of predator-prey pairings including myxobacteria other than
64 *M. xanthus* might provide additional insight into prey resistance to myxobacterial
65 predation. For our predator-prey experiments, the soil dwelling myxobacterium
66 *Cystobacter ferrugineus* strain Cbfe23 was included due to a favorable growth profile and
67 capability to quickly consume *P. putida* during standard predation assays (Seccareccia
68 et al., 2015; Akbar et al., 2017; Livingstone et al., 2017). Also found within soils, root
69 colonizing *P. putida* was chosen as prey due to an established ability to resist protozoan
70 grazers (Seiler et al., 2017). Initial predator-prey experiments provided a *P. putida*
71 phenotype capable of avoiding *C. ferrugineus* predation. Herein we report the generation
72 and predator avoidance of a *P. putida* phenotype resistant to myxobacterial predation
73 using standard predator-prey experiments, differential gene expression data comparing
74 the survivor phenotype with predator-unexposed *P. putida*, and traits observed to
75 potentially contribute to predator avoidance.

76 **Results**

77 **Selection of predation resistant *P. putida* phenotype**

78 Utilizing predation assays where an inoculum of *C. ferrugineus* was introduced to the
79 edge of an established spot of *P. putida* (Seccareccia et al., 2015), we considered
80 swarming overtaking the *P. putida* spot with no visible prey remaining to be an endpoint
81 for assessment of viable prey cells using colony forming unit (CFU) assays. Typically, *C.*

82 *ferrugineus* swarmed predation sensitive *P. putida* with no visible prey after 3 days of co-
83 cultivation on nutrient restrictive WAT agar (Figure 1A and 1D). However, from 100 total
84 assays 5 provided minimally consumed and readily observable *P. putida* remaining after
85 10-14 days (Figure 1B and 1D). Additionally, instead of frontal attack at the predator-prey
86 interface when exposed to predation sensitive *P. putida*, *C. ferrugineus* swarmed the
87 perimeter of the survivor phenotype (Supplemental Figure 1). Exponentially fewer viable
88 colonies of predation sensitive *P. putida* were observed from endpoint CFU assays (3-4
89 days for predation sensitive *P. putida*; 10-14 days for *P. putida* survivor phenotype)
90 supporting the assumption that swarming resistance correlates with prey survival (Figure
91 1D and 1E). Also apparent from CFU assays, colonies of the survivor phenotype were
92 consistently smaller when compared to predation sensitive *P. putida* (Figure 1C).
93 Predation resistance of the survivor phenotype was also observed from additional
94 predation assays with the optical density of prey inoculum doubled (OD_{600}=1.0 versus
95 OD_{600}=0.5). (Supplemental Figure 2). Stocks of each *P. putida* survivor observed from
96 predation assays were stored at -80°C as individual aliquots and utilized to determine
97 features associated with the survivor phenotype that might contribute to predator
98 avoidance.

99 **Differential gene expression of predator-unexposed *P. putida* and survivor**
100 **phenotype**

101 Utilizing RNA sequencing, we conducted comparative transcriptomic experiments
102 between the predator unexposed (control) *P. putida* and the survivor phenotype (n=3
103 biological replicates with biological replicates for the survivor phenotype defined as an
104 individually observed phenotype resistant to *C. ferrugineus* predation for ≥10 days). This

105 comparative analysis determined that 1,178 genes were down-regulated ≥4-fold and 122
106 genes were up-regulated ≥4-fold across the survivor phenotype replicates when
107 compared to control *P. putida* replicates (n=3; p≤0.05). Considering up-regulated genes
108 from the survivor phenotype with the highest fold change values, apparent differences in
109 overexpressed features specific to the survivor phenotype included genes involved in
110 mucoid conversion, siderophore production, and a variety of membrane-associated
111 proteins (Figure 2A). A 4 gene operon including a ferric uptake regulatory (*furA*)
112 associated gene (WP_016501343.1), a fumarate hydratase (WP_016501342.1), a
113 manganese superoxide dismutase (*sodA*) (WP_016501340.1), and a hypothetical protein
114 with a conserved DUF2753 domain (WP_06501341.1) was significantly up-regulated in
115 the survivor phenotype (Figure 2B and 2C). Expression of this operon from *P. aeruginosa*
116 in response to iron limitation leads to elevated alginate production, an exopolysaccharide
117 composed of mannuronic acid and guluronic acid monomers, and increased mucoidy
118 (Hassett et al., 1997b; Hassett et al., 1997a) and corroborates our observation of small
119 colony variance from the survivor phenotype. Interestingly, the alginate regulatory
120 elements MucA (WP_016498171.1) and MucB (WP_016498172.1) were both
121 significantly down regulated in the survivor phenotype (Figure 2B). The anti-sigma factor
122 MucA and the associated binding partner MucB inhibit mucoid conversion by
123 sequestering the alternative sigma factor AlgU required for alginate production in *P.*
124 *aeruginosa* (Deretic et al., 1993; Martin et al., 1993; Damron and Goldberg, 2012; Li et
125 al., 2019). Increased transcription from this operon combined with decreased transcription
126 of MucA and MucB, indicates that mucoid conversion might contribute to predator
127 avoidance which parallels *P. aeruginosa* predatory avoidance mechanisms when

128 exposed to grazing amoeba (Matz et al., 2004). Also associated with iron limitation,
129 regulatory and biosynthetic genes contributing to production of the siderophore
130 pyoverdine were significantly up-regulated in the survivor phenotype. These included
131 PvdA an L-ornithine monooxygenase (WP_016499102.1) and PvdH a diaminobutyrate-
132 2-oxoketoglutarate transaminase (WP_016498669.1) both involved in pyoverdine
133 precursor biosynthesis, a regulatory transcription factor PvdS (WP_016498655.1), a
134 proximal MbtH-like protein (WP_016499090.1), and a core nonribosomal peptide
135 synthetase homologous to PvdL from *P. aeruginosa* (NP_746359.1) (Supplemental
136 Figure 3) (Drake et al., 2007; Felnagle et al., 2010; Parker et al., 2014; Ringel and Bruser,
137 2018). Also associated with iron limiting conditions, a bacterioferritin-associated
138 ferredoxin (WP_016488781.1) was upregulated in the survivor phenotype. A variety of
139 membrane-associated proteins were also overexpressed in the survivor phenotype
140 including an osmotically inducible protein OsmY (WP_0016501632.1), an outer
141 membrane protein A (OmpA) family protein (WP_016501196.1), an FKBP-type peptidyl-
142 prolyl cis-trans isomerase (WP_0165010671), an aquaporin (WP_016498616.1), and a
143 DUF1282 domain-containing hypothetical protein from the Yip1 superfamily
144 (WP_016499858.1) (Figure 2A). While not a membrane associated feature, we also found
145 the overexpression of a formaldehyde dehydrogenase (WP_016497631.1) by the
146 survivor phenotype to be of note due to the recent observation that suggests
147 formaldehyde secretion to be a predation-resistance trait of *P. aeruginosa* (Sutton et al.,
148 2019). The abundance of up-regulated genes that encode membrane-associated
149 products in the survivor phenotype including those responsible for increased mucoid
150 production provides insight into features involved in predation avoidance. Numerous

151 efflux and transport proteins were also among the most up-regulated genes observed
152 from the survivor phenotype (Figure 2D). Upregulated efflux genes included inner
153 (WP_016498130 and WP_016499477.1) and outer (WP_016498128.1) membrane
154 components highly homologous to the AcrAD-TolC-type multidrug resistance-nodulation-
155 division (RND) family of efflux pumps and the Mex RND efflux pumps known to facilitate
156 *P. aeruginosa* resistance to aminoglycosides and tetracyclines (Aeschlimann, 2003; Li et
157 al., 2015; Garneau-Tsodikova and Labby, 2016). Genes encoding features homologous
158 to multidrug efflux pumps contributing to virulence of human pathogens were also up-
159 regulated in the survivor phenotype including a P-type ATPase (WP_016502100) and an
160 additional RND/MmpL (Mycobacterial membrane protein Large) protein (Figure 2D).
161 Provided theses observed differences in gene expression, we sought to determine if the
162 survivor phenotype demonstrated antibiotic resistance and increased mucoidy, which
163 have both been previously associated with predator avoidance strategies.

164 **Antibiotic resistance of survivor phenotype**

165 Provided the observation that numerous transport proteins were overexpressed in the
166 survivor phenotype (Figure 2D) including RND-type efflux pumps known to contribute to
167 *P. aeruginosa* antibiotic resistances, we were interested to determine if the survivor
168 phenotype exhibited antibiotic resistance. The survivor phenotype was capable of initially
169 forming colonies on LB agar supplemented with the antibiotics gentamicin (10 μg/ml),
170 kanamycin (50 μg/ml), and tetracycline (10 μg/ml), with no colonies from predation
171 sensitive *P. putida* observed on identical medias. Subsequent growth curve assays
172 comparing predation sensitive *P. putida* with the survivor phenotype when grown in LB
173 and LB supplemented with antibiotics (Figure 3A and 3B) confirmed that the survivor

174 phenotype was uniquely resistant to gentamicin, kanamycin, and tetracycline. These
175 results combined with the overexpression of efflux-associated proteins observed from the
176 survivor phenotype confirms that *C. ferrugineus* selection provides prey that benefit from
177 antibiotic resistance and suggests that efflux-mediated antibiotic resistance is a *P. putida*
178 predation avoidance feature.

179 **Increased production of alginate by survivor phenotype**

180 Alginate-based formation of mucoid biofilms has previously been associated with *P.*
181 *aeruginosa* avoidance of the protozoan grazer *Rhynchomonas nasuta* (Matz et al., 2002;
182 Matz et al., 2004; Matz and Kjelleberg, 2005; Matz et al., 2005). Utilizing established
183 carbazole assays on isolated alginate (Knutson and Jeanes, 1968; Al Ahmar et al., 2020),
184 we sought to determine if the increased transcription of genes known to impact alginate
185 production observed from the survivor phenotype resulted in increased production of
186 alginate when compared to predator unexposed *P. putida*. Comparing isolated alginate
187 from predation sensitive *P. putida* with the survivor phenotype, we observed that the
188 survivor phenotype indeed produced more alginate when compared to *P. putida* not
189 exposed to *C. ferrugineus* (Figure 4).

190 **Predation resistance of survivor phenotype in subsequent predation assays**

191 Additional subsequent predation assays were done to assess the predator avoidance trait
192 of the *P. putida* survivor phenotype with *P. putida* not exposed to *C. ferrugineus* included
193 as a control. These predation assays included an assay as previously described with
194 predator cells directly introduced to the edge of established prey, a similar slightly
195 modified assay with predator introduced at a distance of 5-7 mm from an established spot
196 of *P. putida*, and a lawn culture assay (Livingstone et al., 2017) monitoring predator

197 swarming diameters when placed at the center of prey embedded in agar. For direct
198 contact assays, time to complete swarming was recorded. As observed in our prior
199 predator-prey experiments, compared to control *P. putida* the survivor demonstrated
200 significantly increased predator avoidance (Figure 5A). The survivor phenotype also
201 demonstrated resistance to swarming compared to predation sensitive *P. putida* during
202 identical direct-contact predation assays conducted on nutrient-rich VY/2 agar
203 (Supplemental Figure 4) For indirect contact predation assays, time to predator-prey
204 contact and time to complete swarming were recorded. Time to predator-prey contact
205 was between 1-2 days for all samples, and as observed in the directed contact predation
206 assays the survivor phenotype demonstrated increased predator avoidance when
207 compared to control *P. putida* (Figure 5B and 5C). However, no differences between
208 swarming diameters of *C. ferrugineus* grown on lawns of control *P. putida* and the *P.*
209 *putida* survivor phenotype were observed (Figure 5D). These data suggest the *P. putida*
210 survivor phenotype benefits from a predator avoidance trait when subjected to 2 out of 3
211 subsequent predation assays.

212 **Discussion**

213 Building upon previously reported resistance strategies to avoid predatory myxobacteria
214 discovered from predator-prey experiments (DePas et al., 2014; Muller et al., 2014; Perez
215 et al., 2014; Muller et al., 2015; Sutton et al., 2019; Wang et al., 2019; Contreras-Moreno
216 et al., 2020), predation experiments including *C. ferrugineus* and *P. putida* provided a
217 prey phenotype significantly resistant to predation. Traits associated with prey resiliency
218 during bacterial predator-prey interactions remain underexplored despite growing
219 evidence that predatory stress contributes to the development of phenotypic traits

220 associated with persistent clinical pathogens (Erken et al., 2013; Sun et al., 2018; Leong,
221 2020). As an example, clinical isolates of persistent *P. aeruginosa* from cystic fibrosis
222 patients exhibit increased mucoidy and small colony variation as well as efflux-mediated
223 antibiotic resistance (Malone, 2015; Winstanley et al., 2016; Maunders and Welch, 2017).
224 Other human pathogens that have demonstrated overlapping factors involved in both
225 virulence and anti-predation strategies include *Legionella pneumophila*, *Escherichia coli*,
226 *Vibrio cholerae*, *Campylobacter jejuni*, *Listeria monocytogenes*, *Mycobacterium leprae*,
227 and *Yersinia enterocolitica* (Erken et al., 2013; Sun et al., 2018). Overlapping factors thus
228 far observed to be associated with both virulence and predator avoidance include biofilm
229 formation (Matz et al., 2004; Matz et al., 2005; Weitere et al., 2005), quorum signal (Sun
230 et al., 2013) and siderophore (Butt and Thomas, 2017) small molecule biosynthesis, toxin
231 production (Steinberg and Levin, 2007; Lainhart et al., 2009; Chekabab et al., 2013), and
232 expression of transport proteins such as type III and type VI secretion systems (Matz et
233 al., 2008; Riquelme et al., 2016) and antibiotic resistance-associated efflux pumps
234 (Pombinho et al., 2017; Vieira et al., 2017). While the impact of predatory selection on
235 virulence factors have primarily been reported from predator-prey experiments with
236 grazing amoeba, efforts to determine the influence of generalist predators on microbial
237 communities have suggested that bacterial predators also drive adaptation of prey traits
238 that overlap with virulence in bacterial pathogens (Nair et al., 2019). Recently, Nair *et al.*
239 reported that during predator-prey interactions with *E. coli* prey, the predatory
240 myxobacterium *Myxococcus xanthus* selects for 2 traits associated with virulence,
241 mucoidy and increased expression of the outer membrane protease OmpT (Nair et al.,
242 2019). Compared to features associated with bacterial strategies to avoid protozoan

243 predators, prey avoidance of myxobacterial predators remains underexplored. Although
244 predator-prey experiments that utilize myxobacteria with various prey such as *Bacillus*
245 *subtilis* (Muller et al., 2014; Muller et al., 2015; Muller et al., 2016), *E. coli* (Livingstone et
246 al., 2018; Nair et al., 2019), *Sinorhizobium melilotti* (Perez et al., 2014; Contreras-Moreno
247 et al., 2020), *P. aeruginosa* (Sutton et al., 2019), and *Streptomyces coelicolor* (Perez et
248 al., 2011) have been reported, all myxobacterial resistances have been discovered from
249 predator-prey experiments that included the model myxobacterium *M. xanthus*. Utilizing
250 an alternative myxobacterium *C. ferrugineus* provides the opportunity to further compare
251 predatory selection and adaptive prey avoidance strategies.
252 Comparative transcriptomics provided key features up-regulated in the *P. putida* survivor
253 phenotype that overlap with traits associated with *P. aeruginosa* predator avoidance and
254 pathogenicity. Of these, 3 putative RND family transporter components with high
255 homology to the MexAB-OprM and MexCD-OprM efflux systems known to mediate *P.*
256 *aeruginosa* antibiotic resistance were up-regulated in the survivor phenotype
257 (Aeschlimann, 2003; Li et al., 2015). Growth curve analysis determined that the *P. putida*
258 survivor phenotype was indeed resistant to the aminoglycosides kanamycin and
259 gentamicin as well as tetracycline; susceptibility to all 3 of these antibiotics was observed
260 from predator unexposed *P. putida*. Also of note, the multidrug efflux pump CmeABC
261 serves as a survival mechanism for *C. jejuni* when engulfed by the predatory amoeba
262 *Acanthamoeba polyphaga* (Vieira et al., 2017). Several features associated with mucoid
263 conversion were also up-regulated in the survivor phenotype including a 4 gene operon
264 responsible for elevated alginate production in *P. aeruginosa* and the regulatory
265 transcription factors MucA and MucB (Hassett et al., 1997b; Hassett et al., 1997a;

266 Damron and Goldberg, 2012; Li et al., 2019). Adaptive mucoid phenotypes have been
267 previously been observed in response to myxobacterial predation (Nair et al., 2019),
268 amoebal grazing (Matz et al., 2002), macrophages (Miskinyte et al., 2013), and lytic
269 phages (Scanlan and Buckling, 2012). Increased alginate production by the survivor
270 phenotype was confirmed using established carbazole assays. Alginate-based mucoid
271 conversion and biofilm formation have previously been associated with *P. aeruginosa*
272 avoidance of grazing amoeba and could also contribute to the small colony variation
273 observed from our survivor phenotype (Matz et al., 2002; Matz et al., 2004; Matz and
274 Kjelleberg, 2005). These results and the observed alternative predatory pattern of *C.*
275 *ferrugineus* during predator-prey interactions with the survivor phenotype parallel
276 previous observation of mucoid *S. meliloti* phenotypes avoiding *M. xanthus* predation
277 (Perez et al., 2014). Also of note, upregulation of an OmpA family protein observed in
278 the survivor phenotype might also correlate with mucoid conversion as *P. aeruginosa*
279 phenotypes that upregulate expression of OmpA also overproduce alginate (Yang et al.,
280 2018). These results provide clear overlap between features contributing to avoidance of
281 myxobacterial and amoebal predation and also afford additional evidence that the
282 coincidental selection of prey virulence factors reported from amoebal predatory stress
283 (Erken et al., 2013) might also be observed from predator-prey interactions involving
284 myxobacteria. Both efflux-mediated antibiotic resistance and mucoid conversion have
285 also been attributed to virulence of clinical isolates of *P. aeruginosa* (Deretic et al., 1993;
286 Mulcahy et al., 2010; Winstanley et al., 2016; Leong, 2020). Additionally, transcriptomic
287 data provided key features for follow-up investigations to assess any direct impact on
288 predator avoidance including biosynthetic genes involved in pyoverdine biosynthesis and

289 numerous features associated with outer membranes. For example, up-regulation of the
290 pyoverdine biosynthetic pathway and a bacterioferritin-associated ferredoxin observed
291 from the survivor phenotype suggests an iron-depleted predator-prey environment similar
292 to the previously interaction between *M. xanthus* and *Streptomyces coelicolor* (Perez et
293 al., 2011). Enhanced production of the primary myxobacterial siderophore myxochelin by
294 *M. xanthus* contributed to an iron-restrictive environment and triggered production of the
295 pigment actinorhodin from *S. coelicolor.*
296 The survivor phenotype observed to be resistant to *C. ferrugineus* predation was
297 assessed with subsequent predation assays to determine the resiliency of the predator
298 avoidance trait. While comparative transcriptomic data provided insight into key up-
299 regulated features potentially involved in prey survival, down-regulation of 1,178 genes in
300 the survivor phenotype when compared to predator unexposed *P. putida* suggests
301 potentially diminished survivor fitness. Despite this, the survivor phenotype maintained
302 the predator avoidance trait in 2 out of 3 subsequent predation assays. While it is unclear
303 why no significant predator avoidance was observed from lawn culture predation assays,
304 we suspect the introduction of predator to the center of prey lawns as opposed to
305 consistent introduction to the peripheral interface of prey potentially reduce any predator
306 avoidance mechanisms. Predator avoidance observed from direct and indirect contact
307 predation assays and the heterogeneity associated with differences between the growth
308 and metabolism of peripheral cells and central cells of bacterial colonies supports this
309 suspicion (Reyrolle and Letellier, 1979; Jeanson et al., 2015). We anticipate that *P. putida*
310 phenotypes resistant to myxobacterial predation continually subjected to such predatory
311 selection will afford adapted phenotypes for further scrutiny of any resulting mutations

312 and genotypes. Ultimately, these results demonstrate the utility of predator-prey
313 experiments using lesser studied myxobacteria and provide insight into how predatory
314 stress might contribute to adaptive phenotypic diversity of bacterial communities.

315 **Materials and Methods**

316 **Bacterial Strains and Cultivation**

317 The myxobacterium *Cystobacter ferrugineus* strain Cbfe23, DSM 52764 was employed
318 as the predator. *Pseudomonas putida* type strain, ATCC 12633, and the discussed *P.*
319 *putida* survivor phenotype resulted from predation assays with this *P. putida* type strain
320 were included as prey. *C. ferrugineus* was grown on VY/2 solid (1.4% w/v agar, 0.1% w/v
321 $CaCl_2$ * 2 H_2O, 0.5% w/v Baker's yeast, 500 µM vitamin B12) media for 5-7 days. Luria-
322 Bertani (LB) solid (1.5% agar) and liquid media were utilized for the cultivation of *P.*
323 *putida*. Predation experiments were performed on WAT agar (1.5% w/v agar, 0.1% w/v
324 $CaCl_2$, 20 mM HEPES) plates. All bacteria were grown at 30 °C.

325 **Predation assays**

326 Prey spot assay was performed as described by Seccareccia et al. (Seccareccia et al.,
327 2015). Briefly, *P. putida* prey was grown in LB liquid media on a rotary shaker (150 rpm)
328 at 30 °C for 16-18 h. Next, the bacterial cultures were sedimented by centrifugation at
329 4,000 g for 15 min, and the sedimented cells were washed and resuspended in TM buffer
330 (50 mM Tris, pH 7.8, 10 mM $MgSO_4$) to an OD_{600} of 0.5. Then the WAT agar plates were
331 spotted with 150 µl of the freshly prepared bacterial suspensions, and the spots were
332 dried in a laminar flow hood. Finally, *C. ferrugineus* was inoculated at the edge of the prey
333 spot. The assay plates were incubated at 30 °C for 14 days or until the full visible
334 swarming of *C. ferrugineus* on the prey spot. The assay was performed with 100

335 replicates. Any prey spot with visible biomass of *P. putida* after day 14 was considered
336 as survivor phenotype of *P. putida*, and five observed *P. putida* survivor stocks were
337 acquired that remained visible after day 14 of the assay.
338 For subsequent predation assays, *P. putida* predation sensitive (control) and the survivor
339 phenotypes were employed as prey. The direct spot assay was performed as mentioned
340 above. Statistical significance of recorded time to predation reported in was calculated
341 using an unpaired t test with Welch's correction in Prism 7.0d. The subsequent directed
342 contact predation assay was also performed on VY/2 (1.4% w/v agar, 0.1% w/v $CaCl_2$ *
343 2 H_2O, 0.5% w/v Baker's yeast, 500 μM vitamin B12) media as well, considered as
344 nutrient-rich media. For indirect contact spot assay, *C. ferrugineus* was inoculated at a
345 distance of 5-7 mm from the established *P. putida* control and *P. putida* survivor prey
346 spots. Next, time *C. ferrugineus* took to reach the prey spots and the time of its swarming
347 over the spots was recorded. Indirect predation assays were performed with 8 replicates
348 per phenotype. Statistical significance of recorded time to predation reported in days and
349 recorded time to initial contact between *C. ferrugineus* and prey reported in days was
350 calculated using an unpaired t test with Welch's correction in Prism 7.0d.
351 Swarming predation assays were based on established lawn culture methods
352 (Livingstone et al., 2017). In brief, *P. putida* prey phenotypes were grown in LB liquid
353 media for 16-18 h at 30 °C with shaking at 150 rpm. The cultures were then subjected to
354 centrifugation at 4,000 g for 15 min, and the sedimented cells were washed and
355 resuspended in TM buffer (50 mM Tris, pH 7.8, 10 mM $MgSO_4$) to an OD_{600} 0.5. Next, 1
356 ml of the cell suspension was spread onto a 14 cm diameter WAT agar plate and dried to
357 form a uniform prey lawn. Finally, *C. ferrugineus* previously cultured on VY/2 agar media

358 was spotted onto the center of the prey lawn. The assay plates were incubated at 30 °C,
359 and the expansion of the *C. ferrugineus* swarm was measured on day 4. Lawn culture
360 predation assays were performed with 8 replicates per phenotype with replicates from
361 each survivor stock included. All 3 predation assays were performed simultaneously for
362 all replicates. Statistical significance of *C. ferrugineus* swarm diameters reported in
363 millimeters on day 4 was calculated using an unpaired t test with Welch's correction in
364 Prism 7.0d

365 **CFU assays.**

366 The colony forming units (CFU) were calculated as described by DePas *et al.* (DePas et
367 al., 2014). Briefly, after the full swarming of *C. ferrugineus* over the prey spot, the agar
368 slab under the prey spot was excised and suspended in 2 mL phosphate buffer saline
369 (PBS). Next, a dilution series from this solution was inoculated on the LB plates, and the
370 plates were incubated at 30 °C for 18 hr. Then, CFU/mL was calculated from the viable
371 colonies that appeared on the LB plates. Finally, the CFU/mL of the survivor was
372 compared with cfu/mL of the unexposed *P. putida,* considered as a control. Statistical
373 significance of all CFU assays was calculated using an unpaired t test with Welch's
374 correction in Prism 7.0d.

375 **RNA sequencing**

376 Triplicate samples of *P. putida* control and *P. putida* survivor phenotype grown from
377 stocks in LB at 37°C for 18 hr and pelleted via centrifugation were stored in RNA*later*
378 solution for sequencing. The DNA from *P. putida* type strain cells (200 μl) was extracted
379 using MagAttract HMW DNA Kit (Qiagen). The DNA was eluted in 100 uL AE buffer. The
380 concentration of DNA was evaluated (Supplementary Table 1) using the Qubit® dsDNA

381 HS Assay Kit (Life Technologies). The library was prepared using Nextera DNA Flex
382 library preparation kit (Illumina) following the manufacturer's user guide. 50 ng DNA was
383 used to prepare the library. The sample underwent the simultaneous fragmentation and
384 addition of adapter sequences. These adapters are utilized during a limited-cycle (6
385 cycles) PCR in which unique index was added to the sample. Following the library
386 preparation, the final concentration of the library (Supplementary Table 1) was measured
387 using the Qubit® dsDNA HS Assay Kit (Life Technologies), and the average library size
388 (Supplementary Table 1) was determined using the Agilent 2100 Bioanalyzer (Agilent
389 Technologies). The library was diluted (to 6.5 pM) and sequenced paired end for 500
390 cycles using the MiSeq system (Illumina).
391 Total RNA was isolated from triplicate samples of the *P. putida* control, the *P. putida*
392 survivor phenotype from stocks, and the kanamycin resistant phenotype using the
393 RNeasy PowerSoil Total RNA Kit (Qiagen) following the manufacturer's instructions. 400
394 μl cell sample was used for extractions. The concentration of total RNA was determined
395 (Supplementary Table 2) using the Qubit® RNA Assay Kit (Life Technologies). For rRNA
396 depletion, first, 1000 ng of total RNA was used to remove the DNA contamination using
397 Baseline-ZERO™ DNase (Epicentre) following the manufacturer's instructions followed
398 by purification using the RNA Clean & Concentrator-5 columns (Zymo Research). DNA
399 free RNA samples were used for rRNA removal by using RiboMinus™ rRNA Removal Kit
400 (Bacteria; Thermo Fisher Scientific) and final purification was performed using the RNA
401 Clean & Concentrator-5 columns (Zymo Research). rRNA depleted samples were used
402 for library preparation using the KAPA mRNA HyperPrep Kits (Roche) by following the
403 manufacturer's instructions. Following the library preparation, the final concentrations of

404 all libraries (Supplementary Table 2) were measured using the Qubit® dsDNA HS Assay
405 Kit (Life Technologies), and the average library size was determined using the Agilent
406 2100 Bioanalyzer (Agilent Technologies). The libraries were then pooled in equimolar
407 ratios of 0.6 nM, and sequenced paired end for 300 cycles using the NovaSeq 6000
408 system (Illumina). Differential expression between the resulting transcriptomes was
409 calculated from pair-wise analysis of trimmed mean of M-values (TMM) normalized read
410 counts (Dillies et al., 2013) including fold change, counts-per-million (CPM), and
411 associated p-values using the R-package, edgeR (Robinson et al., 2010). Differential
412 expression data with p-values ≤ 0.05 were considered statistically significant. Genome
413 and RNA sequencing was conducted by MR DNA (Molecular Research LP). All fold
414 change, CPM, and associated p-values resulting from differential expression experiments
415 as described included as supplementary data files TABLE 1 (*P. putida* survivor compared
416 with *P. putida* control). All raw RNAseq data is publicly available at the NCBI Sequence
417 Read Archive (PRJNA577468).

418 **Antibiotic Susceptibility Assays.**

419 The standard growth curve assay was employed to determine the sensitivity of the
420 unexposed *P. putida* and the survivor phenotype towards kanamycin (50 mg/mL),
421 gentamicin (10 mg/mL), and tetracycline (10 mg/mL) antibiotics. The Lauria Bertani (LB)
422 broth without any supplemented antibiotics was used as a control. The test was
423 performed in a 96-well microtiter plate. In a 96-well plate, each well having 200 µL of LB
424 or LB supplemented with an antibiotic was inoculated with a colony of *P. putida.* Next, the
425 absorbance at OD_{620} was recorded using a plate reader every 30 min for 10 hr to examine
426 the growth dynamics of each phenotype. The test was performed in 12 replicates per

427 condition for both phenotypes. Recorded OD_{620} values were plotted using Prism version
428 7.0d with error bars depicting standard deviation of replicate data.

429 **Carbazole Assays.**

430 The alginate was isolated according to Jones *et al*. (Jones et al., 2013). In brief, both *P.*
431 *putida* phenotype unexposed to the predatory stress and the survivor phenotype were
432 grown overnight in 2 ml LB media and adjusted to an OD_{600} of 1.00. Following
433 centrifugation, 1 ml of supernatant was treated with 2% cetyl pyridinium chloride to
434 precipitate the alginate. The precipitated alginate was further collected by centrifugation.
435 It was resuspended in 1 M NaCl and then re-precipitated in cold isopropanol. Precipitated
436 alginate was suspended in 150 μl 0.9% (w/v) saline solution. Following established
437 protocols (Knutson and Jeanes, 1968; Al Ahmar et al., 2020), a 50 μL aliquot of the
438 isolated alginate and a dilution series of standard alginic acid (Sigma) were mixed with
439 200 μL of a solution of 25 mM sodium tetraborate in sulfuric acid and added in a 96-well
440 plate. Next, the plate was heated for 10 min at 100 °C in an oven. After cooling at room
441 temperature for 15 min, 50 μl of a 0.125% carbazole solution in absolute ethanol was
442 added. Then, the plate was re-heated at 100 °C for 10 min in an oven and cooled down
443 at room temperature for 15 min. Finally, the plate was read in a microplate reader at a
444 wavelength of 550 nm. Quantities of alginate per sample (μg/ml) were calculated from the
445 resulting standard curve of purchase alginic acid, and statistical significance was
446 calculated using an unpaired t test with Welch's correction in Prism 7.0d.

447 **Author Contributions.**

448 SA performed the experiments. DCS supervised the project. SA and DCS conceived the
449 project, designed the experiments, and wrote the manuscript.

450 **Acknowledgements.**

451 The authors appreciate funding and support from the National Institute of Allergy and
452 Infectious Diseases (R15AI137996) and the National Institute of General Medical
453 Sciences of the National Institutes of Health (P20GM130460). The authors appreciate
454 Scot E. Dowd at MR DNA, Molecular Research LP for assistance throughout sequencing
455 services provided.

456 **References.**

457 Aeschlimann, J.R. (2003) The role of multidrug efflux pumps in the antibiotic resistance of
458 Pseudomonas aeruginosa and other gram-negative bacteria. Insights from the Society of
459 Infectious Diseases Pharmacists. *Pharmacotherapy* **23**: 916-924.
460 Akbar, S., Dowd, S.E., and Stevens, D.C. (2017) Draft Genome Sequence of Cystobacter
461 ferrugineus Strain Cbfe23. *Genome Announc* **5**.
462 Al Ahmar, R., Kirby, B.D., and Yu, H.D. (2020) Culture of Small Colony Variant of Pseudomonas
463 aeruginosa and Quantitation of its Alginate. *J Vis Exp*.
464 Albataineh, H., and Stevens, D.C. (2018) Marine Myxobacteria: A Few Good Halophiles. *Mar*
465 *Drugs* **16**.
466 Butt, A.T., and Thomas, M.S. (2017) Iron Acquisition Mechanisms and Their Role in the Virulence
467 of Burkholderia Species. *Front Cell Infect Microbiol* **7**: 460.
468 Chekabab, S.M., Daigle, F., Charette, S.J., Dozois, C.M., and Harel, J. (2013) Shiga toxins decrease
469 enterohaemorrhagic Escherichia coli survival within Acanthamoeba castellanii. *FEMS Microbiol*
470 *Lett* **344**: 86-93.
471 Contreras-Moreno, F.J., Munoz-Dorado, J., Garcia-Tomsig, N.I., Martinez-Navajas, G., Perez, J.,
472 and Moraleda-Munoz, A. (2020) Copper and Melanin Play a Role in Myxococcus xanthus
473 Predation on Sinorhizobium meliloti. *Front Microbiol* **11**: 94.
474 Damron, F.H., and Goldberg, J.B. (2012) Proteolytic regulation of alginate overproduction in
475 Pseudomonas aeruginosa. *Mol Microbiol* **84**: 595-607.
476 DePas, W.H., Syed, A.K., Sifuentes, M., Lee, J.S., Warshaw, D., Saggar, V. et al. (2014) Biofilm
477 formation protects Escherichia coli against killing by Caenorhabditis elegans and Myxococcus
478 xanthus. *Appl Environ Microbiol* **80**: 7079-7087.
479 Deretic, V., Martin, D.W., Schurr, M.J., Mudd, M.H., Hibler, N.S., Curcic, R., and Boucher, J.C.
480 (1993) Conversion to mucoidy in Pseudomonas aeruginosa. *Biotechnology (N Y)* **11**: 1133-1136.
481 Dillies, M.A., Rau, A., Aubert, J., Hennequet-Antier, C., Jeanmougin, M., Servant, N. et al. (2013)
482 A comprehensive evaluation of normalization methods for Illumina high-throughput RNA
483 sequencing data analysis. *Brief Bioinform* **14**: 671-683.
484 Drake, E.J., Cao, J., Qu, J., Shah, M.B., Straubinger, R.M., and Gulick, A.M. (2007) The 1.8 A crystal
485 structure of PA2412, an MbtH-like protein from the pyoverdine cluster of Pseudomonas
486 aeruginosa. *J Biol Chem* **282**: 20425-20434.

487 Ellis, B.M., Fischer, C.N., Martin, L.B., Bachmann, B.O., and McLean, J.A. (2019) Spatiochemically
488 Profiling Microbial Interactions with Membrane Scaffolded Desorption Electrospray Ionization-
489 Ion Mobility-Imaging Mass Spectrometry and Unsupervised Segmentation. *Anal Chem* **91**: 13703-
490 13711.
491 Erken, M., Lutz, C., and McDougald, D. (2013) The rise of pathogens: predation as a factor driving
492 the evolution of human pathogens in the environment. *Microb Ecol* **65**: 860-868.
493 Felnagle, E.A., Barkei, J.J., Park, H., Podevels, A.M., McMahon, M.D., Drott, D.W., and Thomas,
494 M.G. (2010) MbtH-like proteins as integral components of bacterial nonribosomal peptide
495 synthetases. *Biochemistry* **49**: 8815-8817.
496 Findlay, B.L. (2016) The Chemical Ecology of Predatory Soil Bacteria. *ACS Chem Biol* **11**: 1502-
497 1510.
498 Garneau-Tsodikova, S., and Labby, K.J. (2016) Mechanisms of Resistance to Aminoglycoside
499 Antibiotics: Overview and Perspectives. *Medchemcomm* **7**: 11-27.
500 Hassett, D.J., Howell, M.L., Sokol, P.A., Vasil, M.L., and Dean, G.E. (1997a) Fumarase C activity is
501 elevated in response to iron deprivation and in mucoid, alginate-producing Pseudomonas
502 aeruginosa: cloning and characterization of fumC and purification of native fumC. *J Bacteriol* **179**:
503 1442-1451.
504 Hassett, D.J., Howell, M.L., Ochsner, U.A., Vasil, M.L., Johnson, Z., and Dean, G.E. (1997b) An
505 operon containing fumC and sodA encoding fumarase C and manganese superoxide dismutase is
506 controlled by the ferric uptake regulator in Pseudomonas aeruginosa: fur mutants produce
507 elevated alginate levels. *J Bacteriol* **179**: 1452-1459.
508 Jeanson, S., Floury, J., Gagnaire, V., Lortal, S., and Thierry, A. (2015) Bacterial Colonies in Solid
509 Media and Foods: A Review on Their Growth and Interactions with the Micro-Environment. *Front*
510 *Microbiol* **6**: 1284.
511 Jones, C.J., Ryder, C.R., Mann, E.E., and Wozniak, D.J. (2013) AmrZ modulates Pseudomonas
512 aeruginosa biofilm architecture by directly repressing transcription of the psl operon. *J Bacteriol*
513 **195**: 1637-1644.
514 Justice, S.S., Hunstad, D.A., Cegelski, L., and Hultgren, S.J. (2008) Morphological plasticity as a
515 bacterial survival strategy. *Nat Rev Microbiol* **6**: 162-168.
516 Knutson, C.A., and Jeanes, A. (1968) A new modification of the carbazole analysis: application to
517 heteropolysaccharides. *Anal Biochem* **24**: 470-481.
518 Lainhart, W., Stolfa, G., and Koudelka, G.B. (2009) Shiga toxin as a bacterial defense against a
519 eukaryotic predator, Tetrahymena thermophila. *J Bacteriol* **191**: 5116-5122.
520 Leong, W., Lutz, C., Williams, J., Yan, H.P., Benny, Y.K.Y., Chua, C., Rice, S.A., Givskov, M.,
521 Sanderson-Smith, M., McDougald, D. (2020) *Pseudomonas aeruginosa* isolates co-incubated with
522 *Acanthamoeba castellanii* exhibit phenotypes similar to chronic cystic fibrosis isolates. *bioRxiv*.
523 Li, S., Lou, X., Xu, Y., Teng, X., Liu, R., Zhang, Q. et al. (2019) Structural basis for the recognition of
524 MucA by MucB and AlgU in Pseudomonas aeruginosa. *FEBS J* **286**: 4982-4994.
525 Li, X.Z., Plesiat, P., and Nikaido, H. (2015) The challenge of efflux-mediated antibiotic resistance
526 in Gram-negative bacteria. *Clin Microbiol Rev* **28**: 337-418.
527 Livingstone, P.G., Morphew, R.M., and Whitworth, D.E. (2017) Myxobacteria Are Able to Prey
528 Broadly upon Clinically-Relevant Pathogens, Exhibiting a Prey Range Which Cannot Be Explained
529 by Phylogeny. *Front Microbiol* **8**: 1593.

530 Livingstone, P.G., Millard, A.D., Swain, M.T., and Whitworth, D.E. (2018) Transcriptional changes
531 when Myxococcus xanthus preys on Escherichia coli suggest myxobacterial predators are
532 constitutively toxic but regulate their feeding. *Microb Genom* **4**.
533 Malone, J.G. (2015) Role of small colony variants in persistence of Pseudomonas aeruginosa
534 infections in cystic fibrosis lungs. *Infect Drug Resist* **8**: 237-247.
535 Martin, D.W., Schurr, M.J., Mudd, M.H., and Deretic, V. (1993) Differentiation of Pseudomonas
536 aeruginosa into the alginate-producing form: inactivation of mucB causes conversion to mucoidy.
537 *Mol Microbiol* **9**: 497-506.
538 Matz, C., and Kjelleberg, S. (2005) Off the hook--how bacteria survive protozoan grazing. *Trends*
539 *Microbiol* **13**: 302-307.
540 Matz, C., Deines, P., and Jurgens, K. (2002) Phenotypic variation in Pseudomonas sp. CM10
541 determines microcolony formation and survival under protozoan grazing. *FEMS Microbiol Ecol*
542 **39**: 57-65.
543 Matz, C., Bergfeld, T., Rice, S.A., and Kjelleberg, S. (2004) Microcolonies, quorum sensing and
544 cytotoxicity determine the survival of Pseudomonas aeruginosa biofilms exposed to protozoan
545 grazing. *Environ Microbiol* **6**: 218-226.
546 Matz, C., McDougald, D., Moreno, A.M., Yung, P.Y., Yildiz, F.H., and Kjelleberg, S. (2005) Biofilm
547 formation and phenotypic variation enhance predation-driven persistence of Vibrio cholerae.
548 *Proc Natl Acad Sci U S A* **102**: 16819-16824.
549 Matz, C., Moreno, A.M., Alhede, M., Manefield, M., Hauser, A.R., Givskov, M., and Kjelleberg, S.
550 (2008) Pseudomonas aeruginosa uses type III secretion system to kill biofilm-associated
551 amoebae. *ISME J* **2**: 843-852.
552 Maunders, E., and Welch, M. (2017) Matrix exopolysaccharides; the sticky side of biofilm
553 formation. *FEMS Microbiol Lett* **364**.
554 Miskinyte, M., Sousa, A., Ramiro, R.S., de Sousa, J.A., Kotlinowski, J., Caramalho, I. et al. (2013)
555 The genetic basis of Escherichia coli pathoadaptation to macrophages. *PLoS Pathog* **9**: e1003802.
556 Mohr, K.I. (2018) Diversity of Myxobacteria-We Only See the Tip of the Iceberg. *Microorganisms*
557 **6**.
558 Mulcahy, L.R., Burns, J.L., Lory, S., and Lewis, K. (2010) Emergence of Pseudomonas aeruginosa
559 strains producing high levels of persister cells in patients with cystic fibrosis. *J Bacteriol* **192**: 6191-
560 6199.
561 Muller, S., Strack, S.N., Ryan, S.E., Kearns, D.B., and Kirby, J.R. (2015) Predation by Myxococcus
562 xanthus induces Bacillus subtilis to form spore-filled megastructures. *Appl Environ Microbiol* **81**:
563 203-210.
564 Muller, S., Strack, S.N., Hoefler, B.C., Straight, P.D., Kearns, D.B., and Kirby, J.R. (2014) Bacillaene
565 and sporulation protect Bacillus subtilis from predation by Myxococcus xanthus. *Appl Environ*
566 *Microbiol* **80**: 5603-5610.
567 Muller, S., Strack, S.N., Ryan, S.E., Shawgo, M., Walling, A., Harris, S. et al. (2016) Identification of
568 Functions Affecting Predator-Prey Interactions between Myxococcus xanthus and Bacillus
569 subtilis. *J Bacteriol* **198**: 3335-3344.
570 Munoz-Dorado, J., Marcos-Torres, F.J., Garcia-Bravo, E., Moraleda-Munoz, A., and Perez, J. (2016)
571 Myxobacteria: Moving, Killing, Feeding, and Surviving Together. *Front Microbiol* **7**: 781.

572 Nair, R.R., Vasse, M., Wielgoss, S., Sun, L., Yu, Y.N., and Velicer, G.J. (2019) Bacterial predator-
573 prey coevolution accelerates genome evolution and selects on virulence-associated prey
574 defences. *Nat Commun* **10**: 4301.
575 Parker, D.L., Lee, S.W., Geszvain, K., Davis, R.E., Gruffaz, C., Meyer, J.M. et al. (2014) Pyoverdine
576 synthesis by the Mn(II)-oxidizing bacterium Pseudomonas putida GB-1. *Front Microbiol* **5**: 202.
577 Perez, J., Moraleda-Munoz, A., Marcos-Torres, F.J., and Munoz-Dorado, J. (2016) Bacterial
578 predation: 75 years and counting! *Environ Microbiol* **18**: 766-779.
579 Perez, J., Munoz-Dorado, J., Brana, A.F., Shimkets, L.J., Sevillano, L., and Santamaria, R.I. (2011)
580 Myxococcus xanthus induces actinorhodin overproduction and aerial mycelium formation by
581 Streptomyces coelicolor. *Microb Biotechnol* **4**: 175-183.
582 Perez, J., Jimenez-Zurdo, J.I., Martinez-Abarca, F., Millan, V., Shimkets, L.J., and Munoz-Dorado,
583 J. (2014) Rhizobial galactoglucan determines the predatory pattern of Myxococcus xanthus and
584 protects Sinorhizobium meliloti from predation. *Environ Microbiol* **16**: 2341-2350.
585 Pombinho, R., Camejo, A., Vieira, A., Reis, O., Carvalho, F., Almeida, M.T. et al. (2017) Listeria
586 monocytogenes CadC Regulates Cadmium Efflux and Fine-tunes Lipoprotein Localization to
587 Escape the Host Immune Response and Promote Infection. *J Infect Dis* **215**: 1468-1479.
588 Reyrolle, J., and Letellier, F. (1979) Autoradiographic study of the localization and evolution of
589 growth zones in bacterial colonies. *J Gen Microbiol* **111**: 399-406.
590 Ringel, M.T., and Bruser, T. (2018) The biosynthesis of pyoverdines. *Microb Cell* **5**: 424-437.
591 Riquelme, S., Varas, M., Valenzuela, C., Velozo, P., Chahin, N., Aguilera, P. et al. (2016) Relevant
592 Genes Linked to Virulence Are Required for Salmonella Typhimurium to Survive Intracellularly in
593 the Social Amoeba Dictyostelium discoideum. *Front Microbiol* **7**: 1305.
594 Robinson, M.D., McCarthy, D.J., and Smyth, G.K. (2010) edgeR: a Bioconductor package for
595 differential expression analysis of digital gene expression data. *Bioinformatics* **26**: 139-140.
596 Scanlan, P.D., and Buckling, A. (2012) Co-evolution with lytic phage selects for the mucoid
597 phenotype of Pseudomonas fluorescens SBW25. *ISME J* **6**: 1148-1158.
598 Seccareccia, I., Kost, C., and Nett, M. (2015) Quantitative Analysis of Lysobacter Predation. *Appl*
599 *Environ Microbiol* **81**: 7098-7105.
600 Seiler, C., van Velzen, E., Neu, T.R., Gaedke, U., Berendonk, T.U., and Weitere, M. (2017) Grazing
601 resistance of bacterial biofilms: a matter of predators' feeding trait. *FEMS Microbiol Ecol* **93**.
602 Steinberg, K.M., and Levin, B.R. (2007) Grazing protozoa and the evolution of the Escherichia coli
603 O157:H7 Shiga toxin-encoding prophage. *Proc Biol Sci* **274**: 1921-1929.
604 Sun, S., Kjelleberg, S., and McDougald, D. (2013) Relative contributions of Vibrio polysaccharide
605 and quorum sensing to the resistance of Vibrio cholerae to predation by heterotrophic protists.
606 *PLoS One* **8**: e56338.
607 Sun, S., Noorian, P., and McDougald, D. (2018) Dual Role of Mechanisms Involved in Resistance
608 to Predation by Protozoa and Virulence to Humans. *Front Microbiol* **9**: 1017.
609 Sutton, D., Livingstone, P.G., Furness, E., Swain, M.T., and Whitworth, D.E. (2019) Genome-Wide
610 Identification of Myxobacterial Predation Genes and Demonstration of Formaldehyde Secretion
611 as a Potentially Predation-Resistant Trait of Pseudomonas aeruginosa. *Front Microbiol* **10**: 2650.
612 Vieira, A., Ramesh, A., Seddon, A.M., and Karlyshev, A.V. (2017) CmeABC Multidrug Efflux Pump
613 Contributes to Antibiotic Resistance and Promotes Campylobacter jejuni Survival and
614 Multiplication in Acanthamoeba polyphaga. *Appl Environ Microbiol* **83**.

615 Wang, C., Liu, X., Zhang, P., Wang, Y., Li, Z., Li, X. et al. (2019) Bacillus licheniformis escapes from
616 Myxococcus xanthus predation by deactivating myxovirescin A through enzymatic glucosylation.
617 *Environ Microbiol* **21**: 4755-4772.
618 Weitere, M., Bergfeld, T., Rice, S.A., Matz, C., and Kjelleberg, S. (2005) Grazing resistance of
619 Pseudomonas aeruginosa biofilms depends on type of protective mechanism, developmental
620 stage and protozoan feeding mode. *Environ Microbiol* **7**: 1593-1601.
621 Winstanley, C., O'Brien, S., and Brockhurst, M.A. (2016) Pseudomonas aeruginosa Evolutionary
622 Adaptation and Diversification in Cystic Fibrosis Chronic Lung Infections. *Trends Microbiol* **24**:
623 327-337.
624 Xiao, Y., Wei, X., Ebright, R., and Wall, D. (2011) Antibiotic production by myxobacteria plays a
625 role in predation. *J Bacteriol* **193**: 4626-4633.
626 Yang, F., Gu, J., Zou, J., Lei, L., Jing, H., Zhang, J. et al. (2018) PA0833 Is an OmpA C-Like Protein
627 That Confers Protection Against Pseudomonas aeruginosa Infection. *Front Microbiol* **9**: 1062.
628

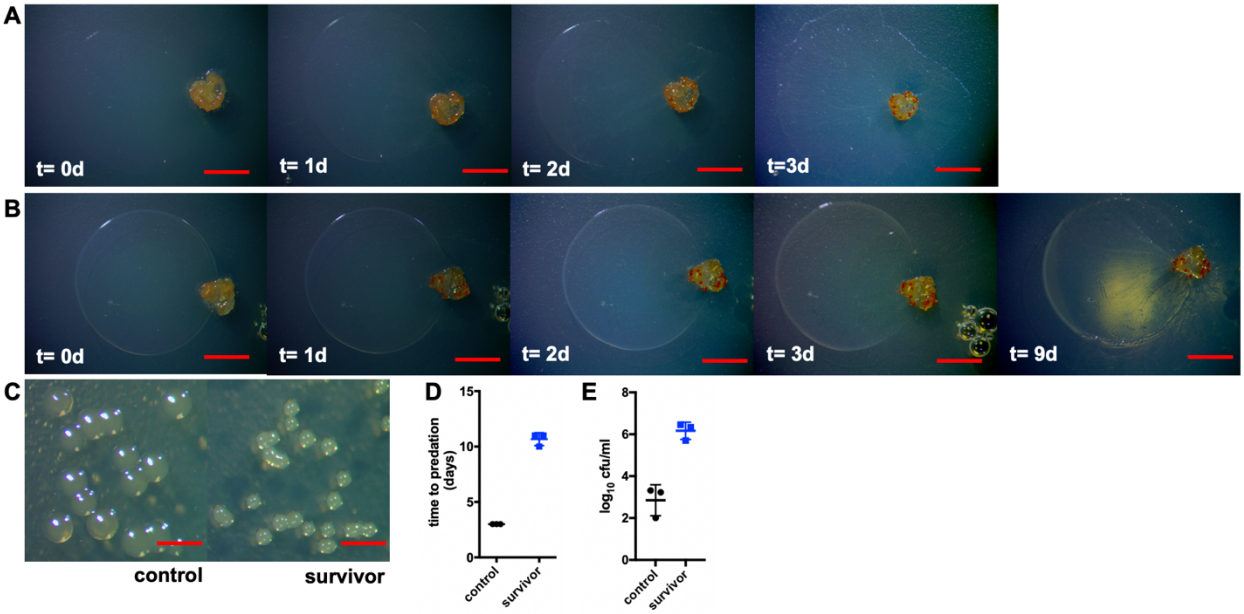

Figure 1: A) 4 day sequence of *C. ferrugineus* predation of *P. putida* with complete swarming of prey (t= d3). B) 4 day sequence depicting predator avoidance observed from *P. putida* survivor phenotype including an additional image from day 9 to demonstrate length of avoidance. C) Comparison of colony sizes of predator unexposed *P. putida* (left) and *P. putida* survivor phenotype (right) depicting small colony variance of the survivor phenotype. D) Time to predation data for *P. putida* control and *P. putida* survivor phenotype (n=3; $p \leq 0.002$) with E) end point colony forming unit data (n=3; $p \leq 0.006$) to determine differences in cell viabilities post-swarming. Unpaired t-test with Welch's correction used for statistical analyses included in D and E; all scale bars depict 1mm.

639

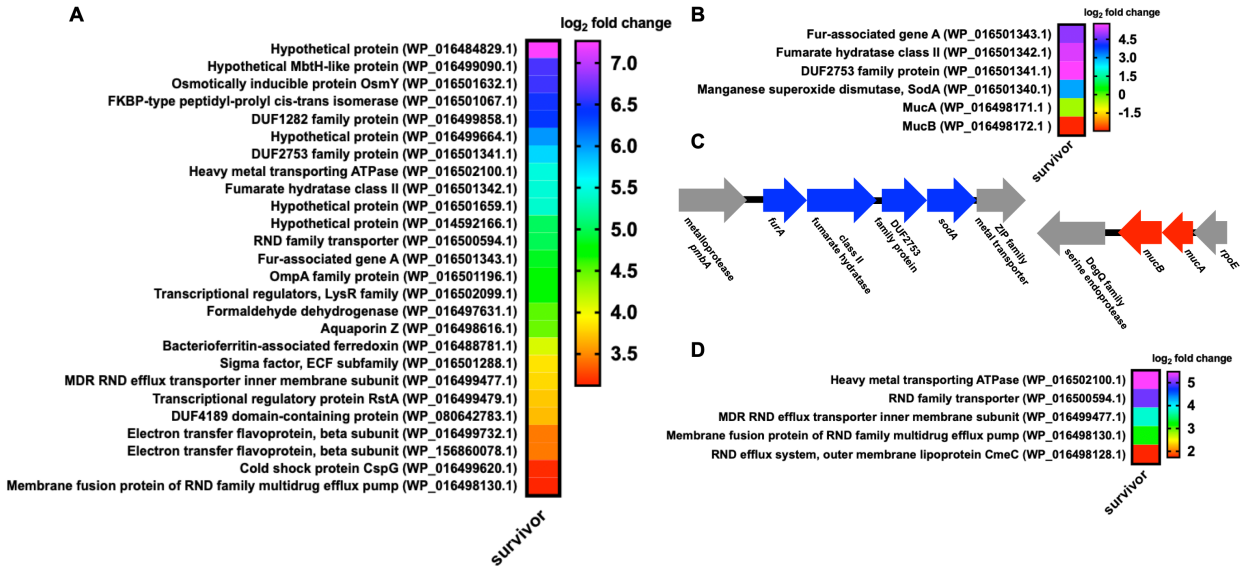

640 **Figure 2:** A) Most abundantly over-expressed genes from survivor phenotype when
641 compared to predator unexposed *P. putida*. B) Up-regulated features associated with
642 alginate production and the associated genomic context for each (C). D) Up-regulated
643 transport proteins including those associated with antibiotic efflux. All data depicted as an
644 averages from 3 biological replicates ($p \leq 0.05$).

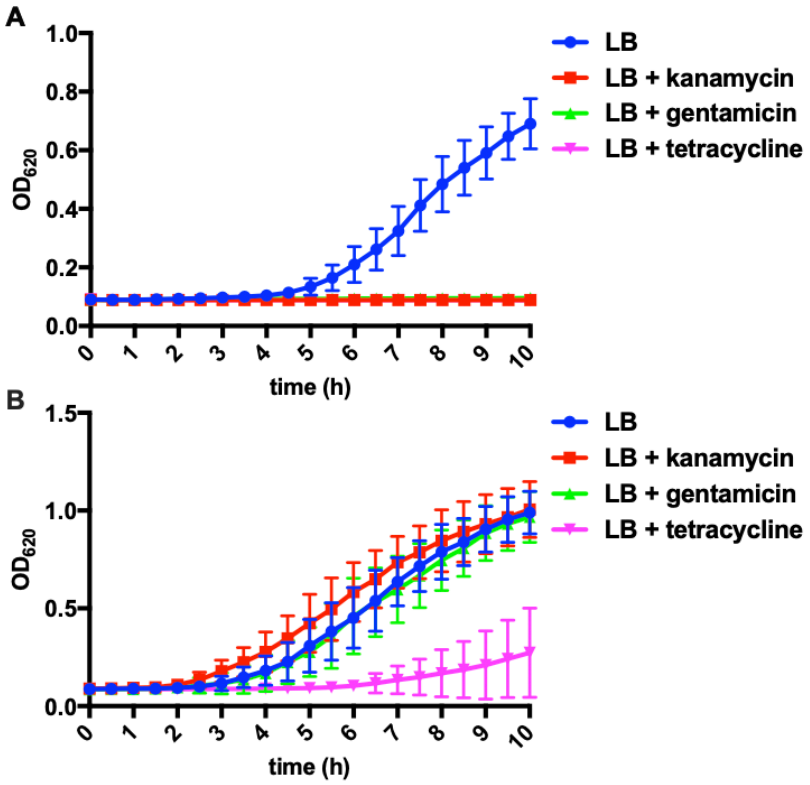

Figure 3: Growth curves for predator unexposed *P. putida* (A) and *P. putida* survivor phenotype (B) depicting antibiotic resistance unique to the survivor phenotype (n=12). LB supplemented with gentamicin (10 μg/ml), kanamycin (50 μg/ml), and tetracycline (10 μg/ml) where indicated.

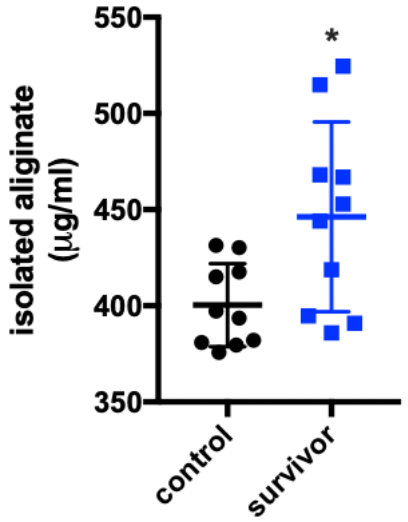

649 **Figure 4:** Isolated alginate concentration determined from carbazole assays depicting
650 increased alginate production observed from the survivor phenotype (n=10; p≤0.02).
651 Relative units determined from average of control values with statistical significance
652 calculated from an unpaired t test with Welch's correction.

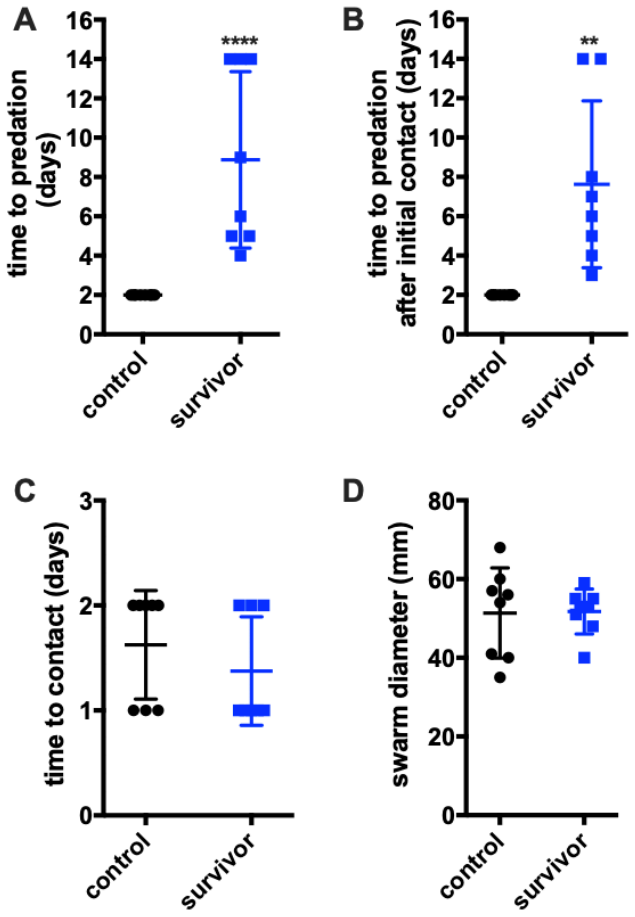

Figure 5: A) Direct contact predation assay as depicted in Figure 1 comparing control (predator unexposed) *P. putida* with freezer stocks of the survivor phenotype (biological replicates) (n=8; p≤0.0001). B) Modified indirect contact predation assay with prey introduced 2 cm from predator (n=8; p≤0.01) and time to predator-prey contact recorded (C). Swarming assays with *C. ferrugineus* plated on prey lawns and swarming diameters recorded after 7 days (n=8). Statistical significance calculated using an unpaired t test with Welch's correction.

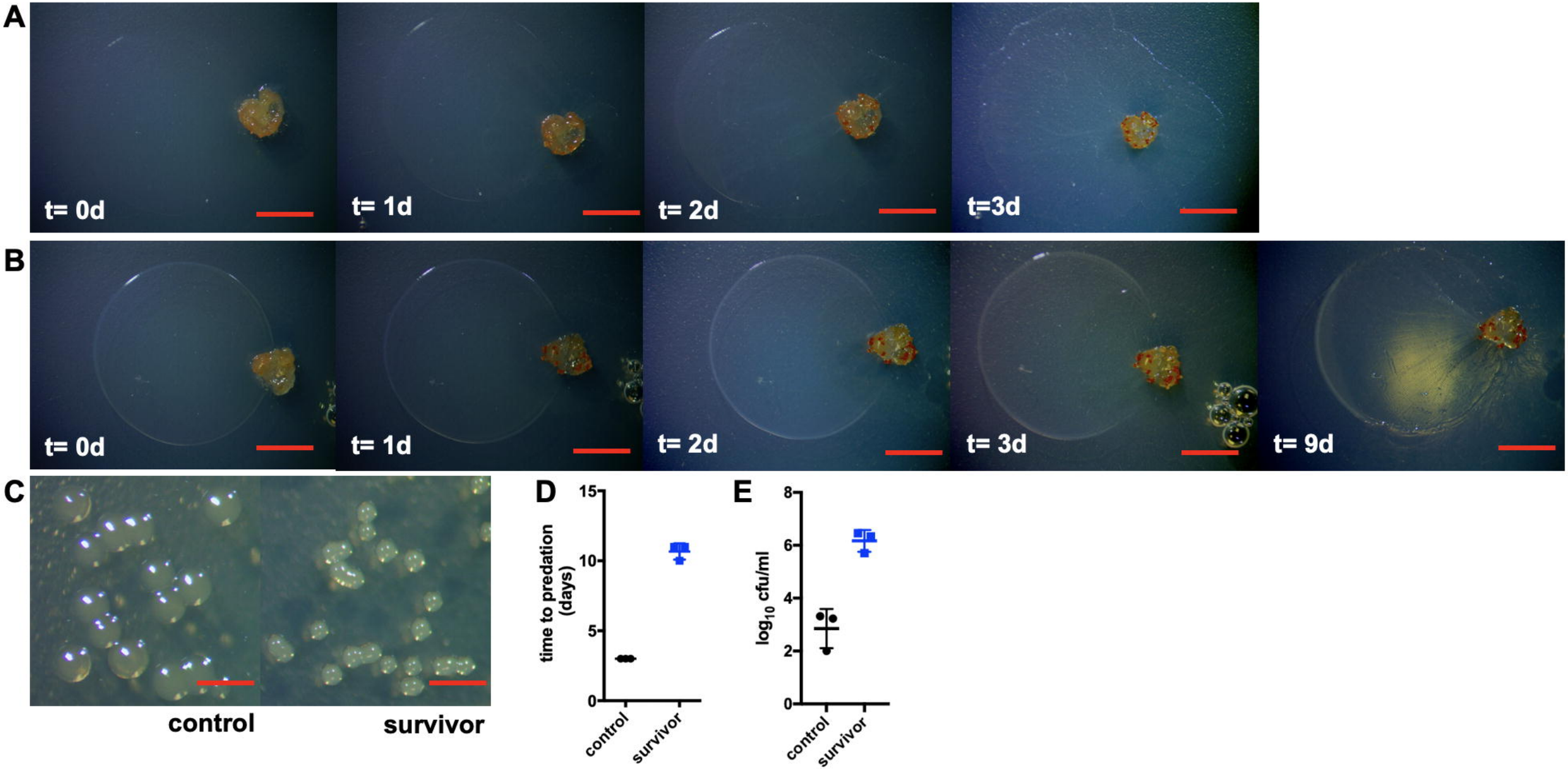
A
t= 0d
t= 1d
t= 2d
t=3d
B
t= 0d
t= 1d
t= 2d
t= 3d
t= 9d
C
control
survivor
D
time to predation (days)
15
10
5
0
control
survivor
E
log10 cfu/ml
8
6
4
2
0
control
survivor

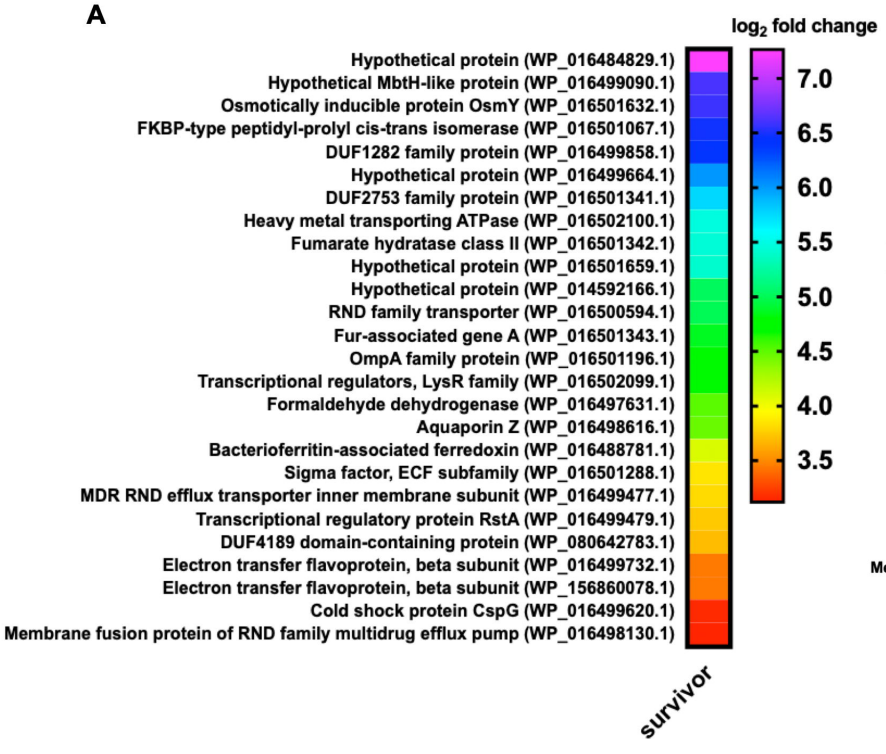
A
log2 fold change
Hypothetical protein (WP_016484829.1)
Hypothetical MbtH-like protein (WP_016499090.1)
Osmotically inducible protein OsmY (WP_016501632.1)
FKBP-type peptidyl-prolyl cis-trans isomerase (WP_016501067.1)
DUF1282 family protein (WP_016499858.1)
Hypothetical protein (WP_016499664.1)
DUF2753 family protein (WP_016501341.1)
Heavy metal transporting ATPase (WP_016502100.1)
Fumarate hydratase class II (WP_016501342.1)
Hypothetical protein (WP_016501659.1)
Hypothetical protein (WP_014592166.1)
RND family transporter (WP_016500594.1)
Fur-associated gene A (WP_016501343.1)
OmpA family protein (WP_016501196.1)
Transcriptional regulators, LysR family (WP_016502099.1)
Formaldehyde dehydrogenase (WP_016497631.1)
Aquaporin Z (WP_016498616.1)
Bacterioferritin-associated ferredoxin (WP_016488781.1)
Sigma factor, ECF subfamily (WP_016501288.1)
MDR RND efflux transporter inner membrane subunit (WP_016499477.1)
Transcriptional regulatory protein RstA (WP_016499479.1)
DUF4189 domain-containing protein (WP_080642783.1)
Electron transfer flavoprotein, beta subunit (WP_016499732.1)
Electron transfer flavoprotein, beta subunit (WP_156860078.1)
Cold shock protein CspG (WP_016499620.1)
Membrane fusion protein of RND family multidrug efflux pump (WP_016498130.1)
7.0
6.5
6.0
5.5
5.0
4.5
4.0
3.5
survivor
B
log2 fold change
Fur-associated gene A (WP_016501343.1)
Fumarate hydratase class II (WP_016501342.1)
DUF2753 family protein (WP_016501341.1)
Manganese superoxide dismutase, SodA (WP_016501340.1)
MucA (WP_016498171.1)
MucB (WP_016498172.1)
4.5
3.0
1.5
0
-1.5
survivor
C
metalloprotease pmbA
furA
fumarate hydratase class II
DUF2753 family protein
sodA
ZIP family metal transporter
DegQ family serine endoprotease
mucB
mucA
rpoE
D
log2 fold change
Heavy metal transporting ATPase (WP_016502100.1)
RND family transporter (WP_016500594.1)
MDR RND efflux transporter inner membrane subunit (WP_016499477.1)
Membrane fusion protein of RND family multidrug efflux pump (WP_016498130.1)
RND efflux system, outer membrane lipoprotein CmeC (WP_016498128.1)
5
4
3
2
survivor

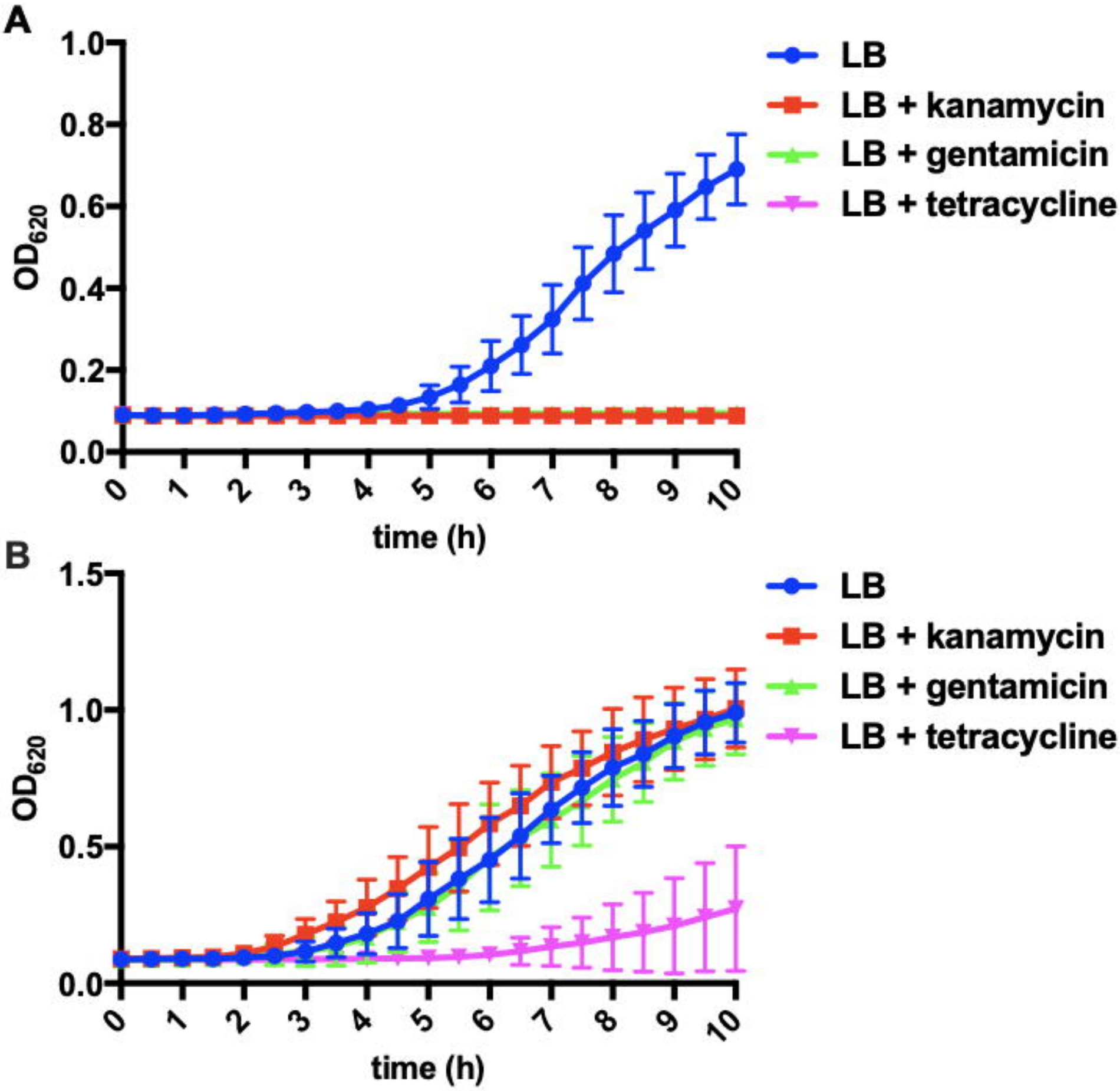
A
1.0
0.8
0.6
0.4
0.2
0.0
OD_{620}
0
1
2
3
4
5
6
7
8
9
10
time (h)
LB
LB + kanamycin
LB + gentamicin
LB + tetracycline
B
1.5
1.0
0.5
0.0
OD_{620}
0
1
2
3
4
5
6
7
8
9
10
time (h)
LB
LB + kanamycin
LB + gentamicin
LB + tetracycline

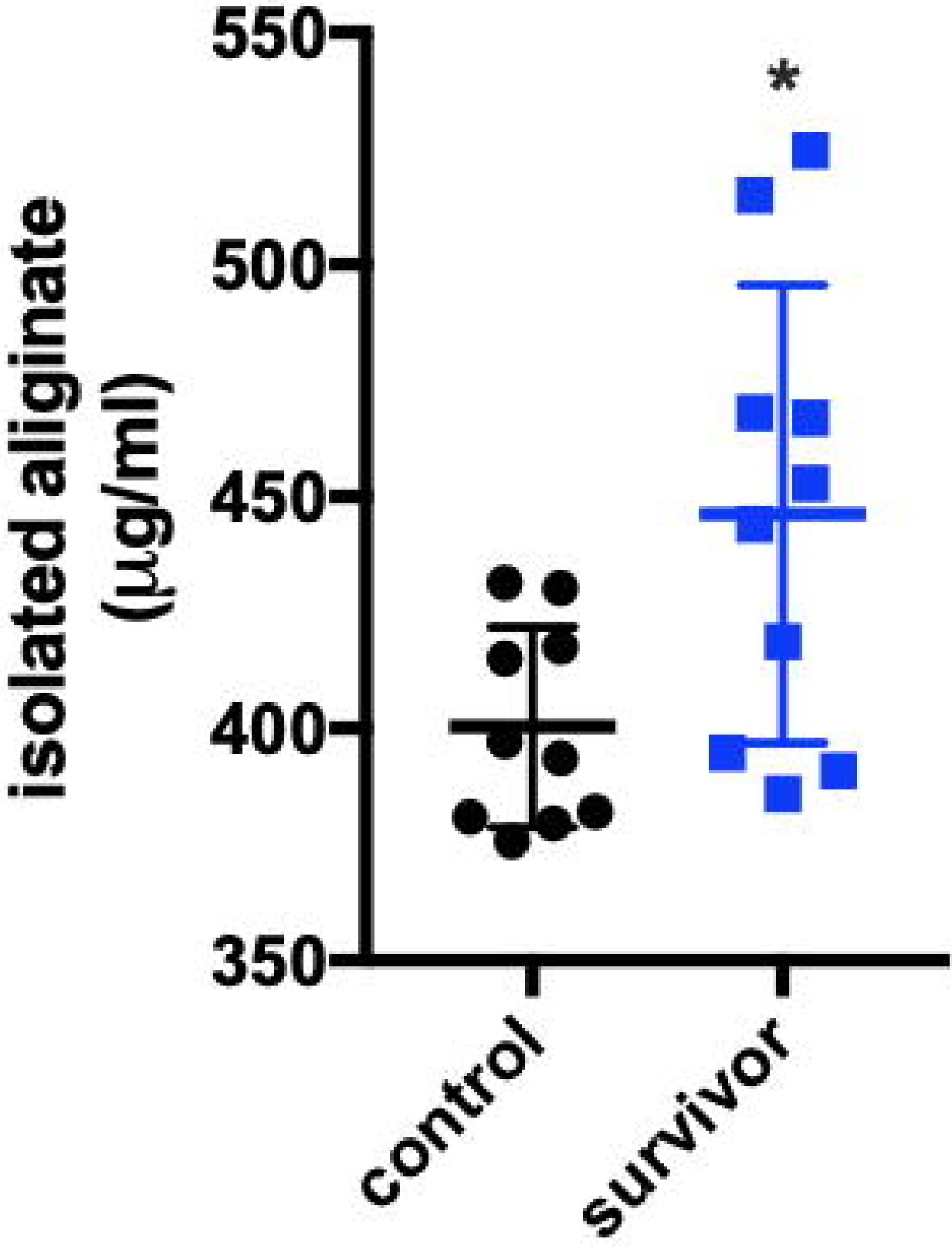
isolated aliginate
(µg/ml)
550
500
450
400
350
*
control
survivor

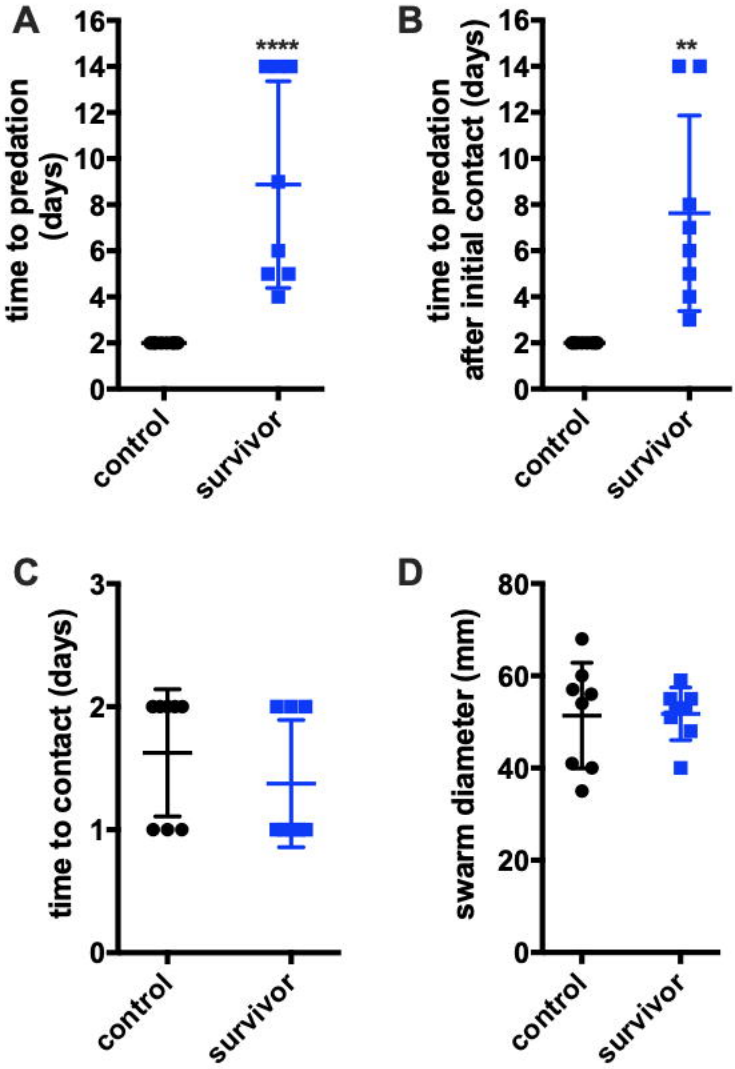
A
time to predation (days)
16
14
12
10
8
6
4
2
0
****
control
survivor
B
time to predation after initial contact (days)
16
14
12
10
8
6
4
2
0
**
control
survivor
C
time to contact (days)
3
2
1
0
control
survivor
D
swarm diameter (mm)
80
60
40
20
0
control
survivor